Electronic Supplementary Material (ESI) for ChemComm.

Photo-enhanced electrocatalytic hydrogen evolution reaction coupled semiconductor with plasma in neutral solution

Congcong Xu[a], Pengfei Cao[a], Nan Wang[a], Houyi Ma[a, *], Meng Lin[a, *]

[a] Key Laboratory for Colloid and Interface Chemistry of State Education Ministry, School of Chemistry and Chemical Engineering, Shandong University, Jinan 250100, China

* Corresponding author: mlin@sdu.edu.cn (M. Lin); hyma@sdu.edu.cn (H. Ma)

Experimental section

Materials and reagents

Potassium chloride (KCl), Zinc chloride ($ZnCl_2$), sodium dihydrogen phosphate (NaH_2PO_4), disodium hydrogen phosphate (Na_2HPO_4), sulphuric acid (H_2SO_4), hydrogen peroxide (H_2O_2), ethanol (CH_3CH_2OH) purchased from Shanghai Sinopharm Reed Co Ltd., (China). Tetrachloroauric (III) acid hydrate ($HAuCl_4 \cdot 4H_2O$), ruthenium trichloride ($RuCl_3$) purchased from Shanghai Aladdin Reagent Co. Indium Tin Oxide (ITO) conductive glass purchased from South China Xiangcheng Technology Co Ltd. All chemicals were analytically pure reagents, and ultrapure water ($\geqslant$18 MΩ) was used throughout the experiments.

Characterization

The morphology and surface structure of the nanomaterials were characterized by field emission scanning electron microscopy (FESEM, JSM-7600F). The morphologies and microstructures of the obtained material were characterized by a

JEOL-JEM-1011-typetransmission electron microscope with an acceleration voltage of 100 kV. The chemical composition of the composites was recorded by X-ray diffraction (XRD) (Rigaku MiniFlex 600, Japan) diffractometer and X-ray photoelectron spectroscopy (XPS, PerkinElmer PHI 5300 system). UV-vis absorption spectra were obtained on the Thermo Evolution 220 ultraviolet-visible spectrometer. The room photoluminescence (PL) spectra (excited by 325 nm illumination) were record on a RenishawRM3000 Micro-Raman system. The time-resolved PL (TRPL) decay spectra were recorded on an Edinburgh instrument as LifeSpec II. The experiments were conducted with a light source of pls-sxe300 xenon lamp, which has a power of 300W. All electrochemical measurements were carried out using a CHI 750E electrochemical workstation (Shanghai Instrument Co., China).

Preparation of AuRu/ZnO NRs/ITO composite structures

ZnO NRs were synthesized by a slight improvement according to the previous report[1]. Prior to the electrodeposition, The ITO conductive glass (0.8×5 cm^2) was soaked in piranha solution (H_2SO_4 : H_2O_2 = 3 : 1) for 30 min and then ultrasonically rinsed three times with ultrapure water. The electrolyte was a 1 mmol L^{-1} $ZnCl_2$ and 2 mol L^{-1} KCl ultrapure aqueous solution, saturated with bubbling oxygen for 20 min. The applied potential was operated at -1 V versus saturated calomel electrode (SCE) for 40 min and the deposition was conducted at a temperature of 80 ℃. To improve the crystallinity and stability, the prepared ZnO was cauterized at 350 °C for 10 min.

AuRu nanoparticles were electrochemically deposited in a 0.1 mol L^{-1} KCl aqueous solution containing 1 mmol L^{-1} $HAuCl_4$ and 1 mmol L^{-1} $RuCl_3$ by

chronoamperometry at -0.2 V for 30 s. The AuRu nanoparticles were aggregated onto the surface of a working electrode of ZnO NRs array parallel to a counter electrode of the Pt plate and a SCE was used as a reference electrode. The prepared AuRu/ZnO NRs/ITO were rinsed three times with deionized water and ethanol respectively.

Electrochemical measurement

Electrochemical measurements were performed with a standard three-electrode setup using a SCE as a reference electrode, a graphite rod as a counter electrode, ITO conductive glass deposited with AuRu/ZnO NRs as a working electrode. All measurements were carried out in a 0.2 mol L^{-1} phosphate buffer solution at pH = 7. A Xe lamp was used as the light source, which emitted simulated sunlight that was directed at the working electrode. Evaluation of the hydrogen precipitation performance by linear scanning voltammetry (LSV). The Electrochemical impedance spectroscopy (EIS) measurements were carried out at 200 mV overpotential in the frequency range from 100 kHz to 10 mHz, which fitting circuit diagram is shown in Figure S7. The electrochemical stability of the catalyst was evaluated by cycling the electrodes 1000 times. Performance comparison with and without the presence of light was evaluated by the chronoamperometry curve. All potentials were referenced to a reversible hydrogen electrode (RHE) converted by using the formula: $E_{RHE} = E_{SCE} + 0.241 + 0.0591\ pH$[2].

Results and discussion

Figure S1 shows the morphological comparison at different concentrations of noble metal ions after electrodeposited for 50 s. The ZnO NRs etching becomes more severe with increasing noble metal concentration. Meanwhile, when the concentration is low, few AuRu nanoparticles were loaded, which may affect the subsequent electrochemical performance. Different deposition time at a constant noble metal ion concentration (1 mmol L^{-1}) was exported, and the morphology of the nanorods is illustrated in Figure S2. The AuRu nanoparticles are uniformly distributed and the nanorod shape is still maintained in a short deposition time (Figure S2a and b). But under a deposition time of 100 s (Figure S2c), the nanorod structure is disrupted, exhibiting a hollow nanotube structure (illustration). When the deposition time reaches 200 s (Figure S2d), the nanorod structure is almost completely broken. The reason for this phenomenon is that the higher energy and unstable crystalline surfaces of the ZnO are preferentially etched by hydrogen or hydroxide ions and electrochemical stresses on the more energetic internal surface[3]. During the electrochemical reduction, the pH value of the electrolyte gradually decreases causing the unstable crystal planes of the ZnO to be selectively etched[4, 5].

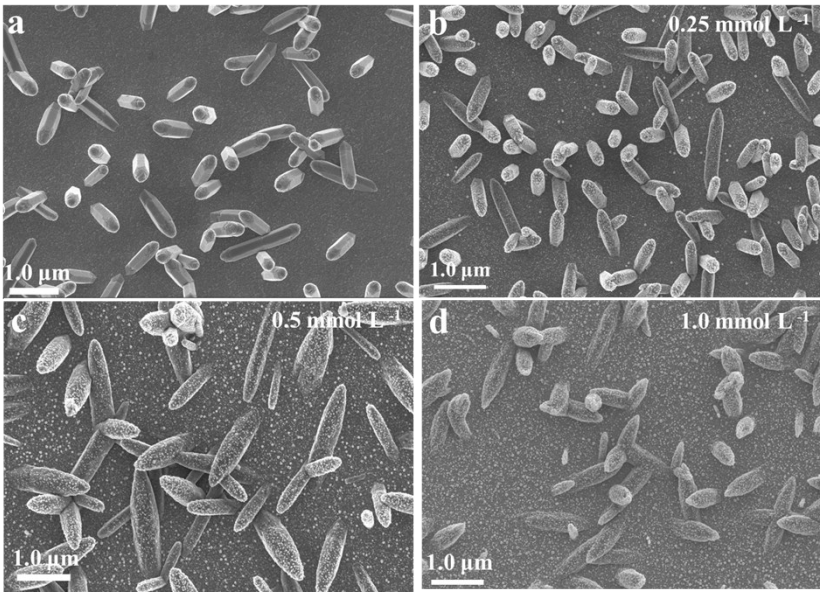

Figure S1. (a) SEM image of ZnO NRs. (b) (c) and (d) SEM images of the electrochemical deposited AuRu/ZnO NRs/ITO under different noble metal concentrations for 50 s.

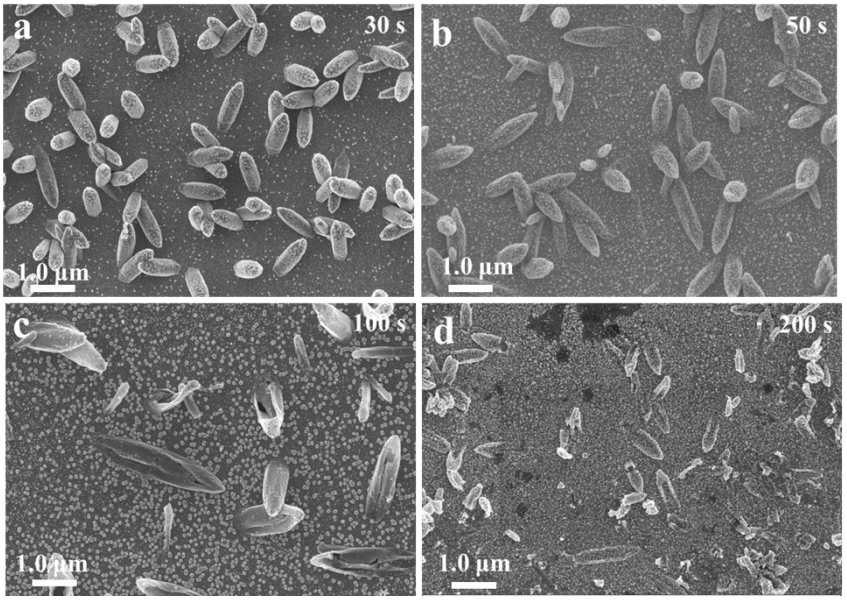

Figure S2. SEM images of the electrochemical deposited AuRu/ZnO NRs/ITO at 1 mmol L^{-1} noble metal concentration with different deposition times.

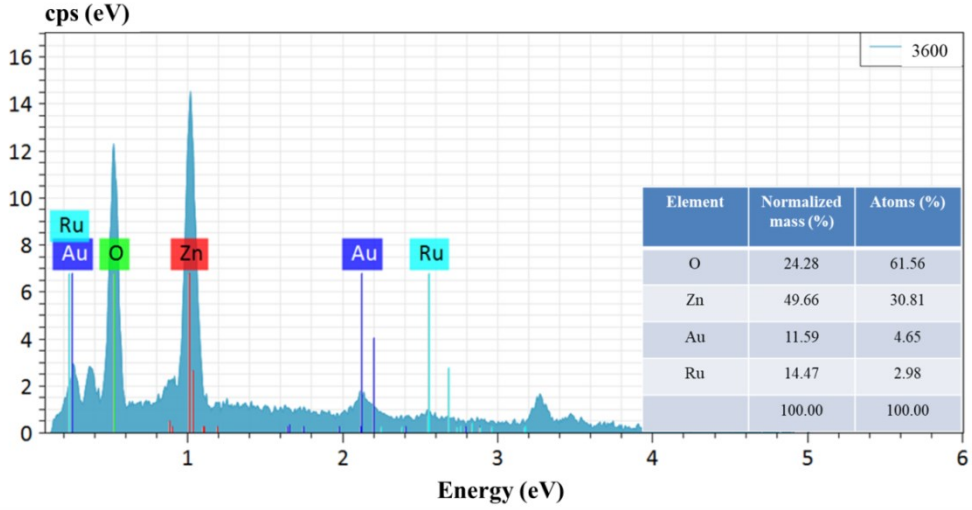

Figure S3. EDS spectrum of the AuRu/ZnO NRs/ITO.

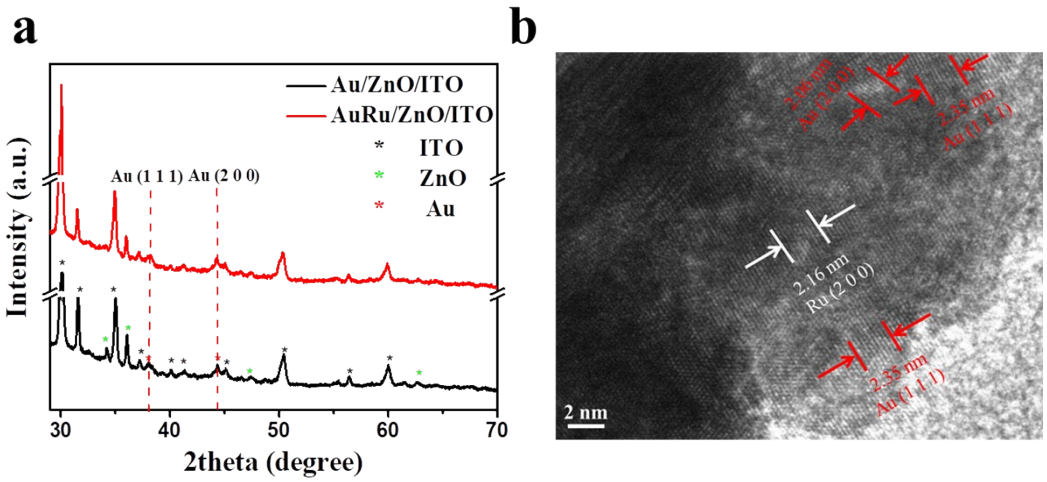

Figure S4. XRD patterns of ZnO NRs/ITO, Au/ZnO NRs/ITO and AuRu/ZnO NRs/ITO.

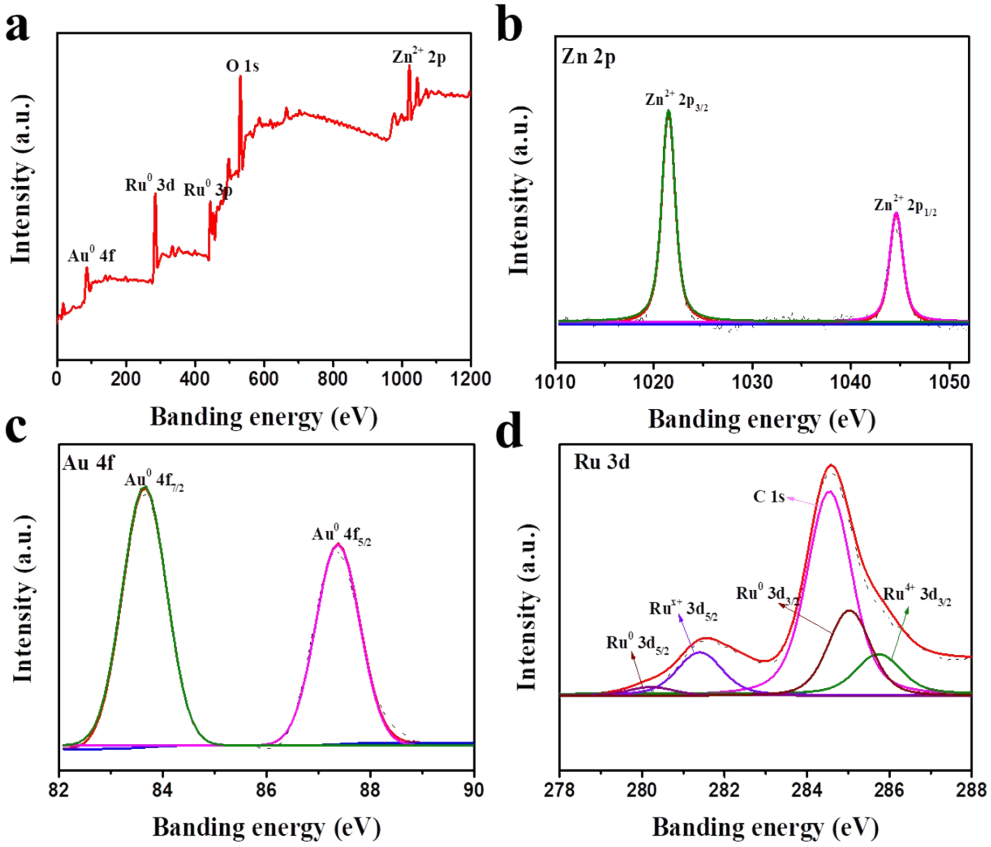

Figure S5. (a) XPS survey spectrum of AuRu/ZnO NRs/ITO. High-resolution XPS spectra of Zn^{2+} 2p (b), Au^{0}4f (c) and Ru^{0}3d (d).

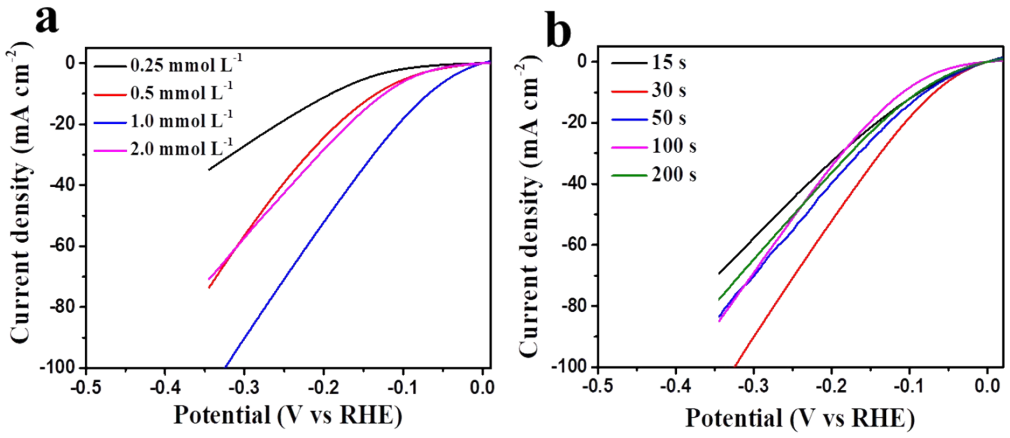

Figure S6. Comparison of electrocatalytic HER performance under different synthesis conditions.

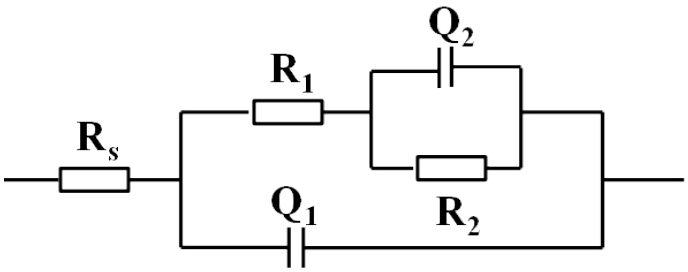

Figure S7. Equivalent circuit diagram for EIS test.

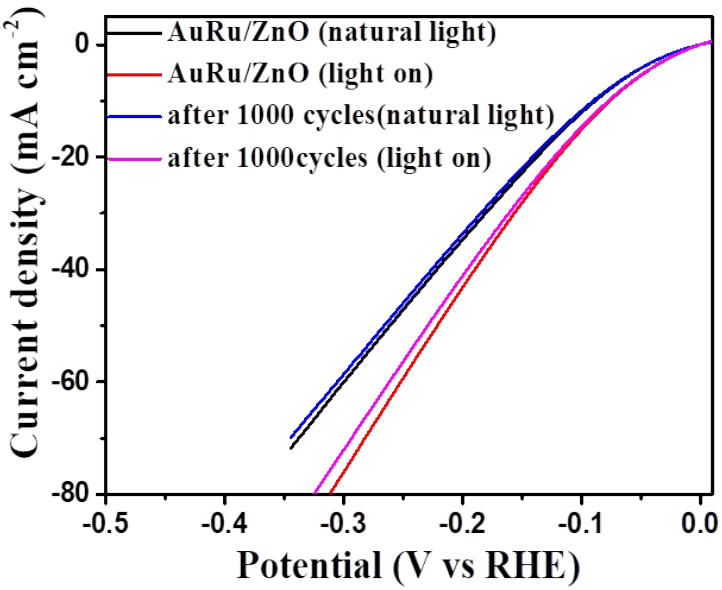

Figure S8. Durability test of the AuRu/ZnO NRs/ITO for 1000 cycles.

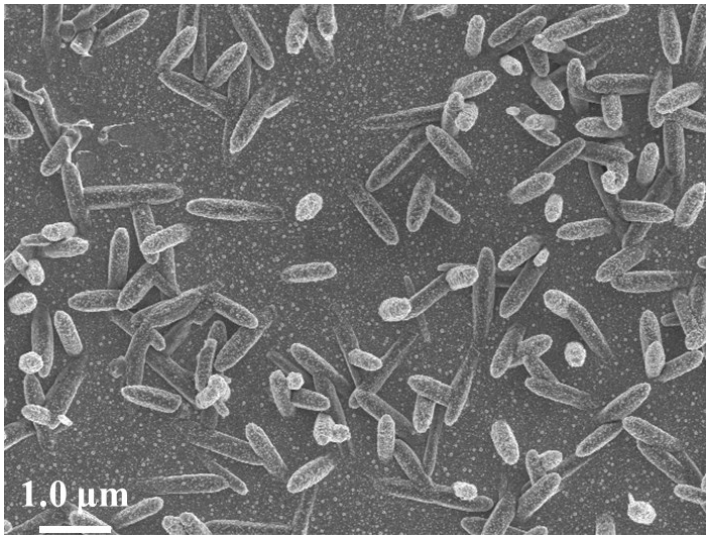

Figure S9. SEM image of the AuRu/ZnO NRs/ITO after 1000 cycles.

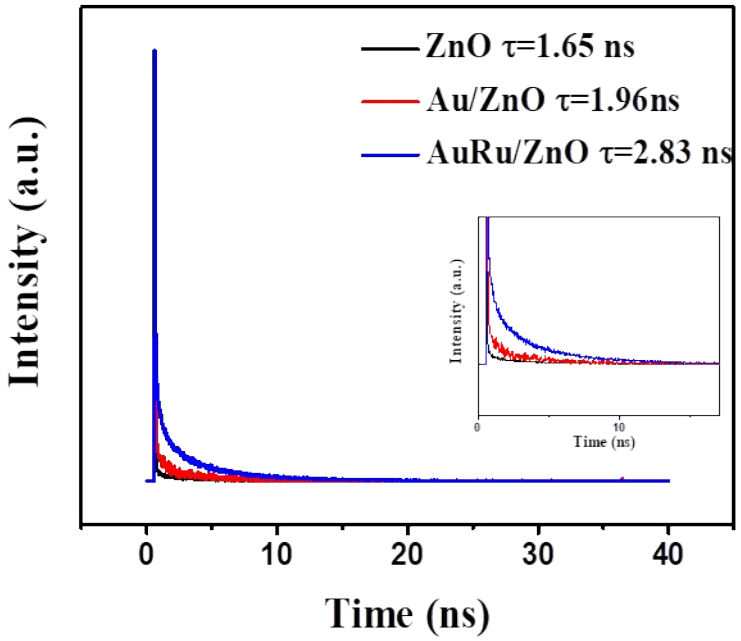

Figure S10. Time-resolved PL decay spectroscopy of ZnO/ITO, Au/ZnO/ITO and AuRu/ZnO/ITO.

Table S1 Corresponding overpotential at 10mA cm^{-2} for different catalysts.

Catalysts	η_{10} (mV)	Refs
RuP_2	179.6	6
Pd/m-TiO_2	197	7
Ni-NiO clusters	230	8
NiP_X	122	9
Ru-s-Sb/antimonene	153	10
MoP700	176	11
AuRu/ZnO NRs/ITO (natural light)	138	This work
AuRu/ZnO NRs/ITO (light on)	112	This work

References

1. M. Lin, RSC Adv., 2015, 5, 9848-9851.
2. L. L. Shen, G. R. Zhang, S. Miao, J. Y. Liu and B. Q. Xu, ACS Catal., 2016, 6, 1680-1690.
3. X. Y. Gan, X. M. L, X. D. Gao and W. D. Yu, J. Alloys Compd., 2009, 481, 397-401.
4. J. Elias, R. Tena-Zaera, G. Y. Wang, and C. Lévy-Clément, Chem. Mater., 2008, 20, 6633-6637.
5. Y. Xie, Y. N. Lv, F. Xu, Y. F. Liu and M. Dai, J. Chin. Ceram. Soc., 2010, 38, 1059-1063.
6. S. Li, M. J. Huang, Y. W. Zhou, X. N. Chen, S Yang and J. Y. Zhu, et al., Chem. Commun., 2019, 55, 10884- 10887.
7. X. J. Zeng, Y. C. Bai, S. M. Choi, L. J. Tong, R. M. Aleisa and Z. W. Li, et al., Mater. Today Nano, 6, 2019, 100038.
8. M. X. Chen, J. Qi, W. Zhang, and R. Cao, Chem. Commun., 2017, 53, 5507-5510.
9. H. L. Jiang, Y. X. Lin, B. X. Chen, Y. K. Zhang, H. J. Liu and X. Z. Duan, et al., Mater. Today, 21, 2018, 602-610.
10. Y. Li, J. X. Chen, J. H. Huang, Y. Hou, L. C. Lei, W. Z. Lin and Y. P. Lian, et al.,Chem. Commun., 2019, 55, 10884-10887.
11. X. H. Xie, M. Song, L. G. Wang, M. H. Engelhard, L. L. Luo and A. Miller, et al., ACS Catal. 2019, 9, 8712−8718.